Genomic data of different resolutions reveal consistent inbreeding estimates but contrasting homozygosity landscapes for the threatened Aotearoa New Zealand hihi

Laura Duntsch[1] - Annabel Whibley[1] - Patricia Brekke[2] - John G. Ewen[2] - Anna W. Santure[1]

Email address of corresponding author Laura Duntsch: ldun612@aucklanduni.ac.nz

[1] School of Biological Sciences, University of Auckland, Auckland, New Zealand

[2] Institute of Zoology, Zoological Society of London, Regents Park, London, United Kingdom

Abstract

Inbreeding can lead to a loss of heterozygosity in a population, and, when combined with genetic drift, may reduce the adaptive potential of a species. However, there is uncertainty about whether resequencing data can provide accurate and consistent inbreeding estimates. Here, we perform an in-depth inbreeding analysis for hihi (*Notiomystis cincta*), an endemic and nationally vulnerable passerine bird of Aotearoa New Zealand. We first focus on subsampling variants from a reference genome male, and find that low-density datasets tend to miss runs of homozygosity (ROH) in some places and overestimate ROH length in others, resulting in contrasting homozygosity landscapes. Low-coverage resequencing and 50K SNP array densities can yield comparable inbreeding results to high-coverage resequencing approaches, but the results for all datasets were highly dependent on the software settings employed. Secondly, we extended our analysis to ten hihi where low-coverage whole genome resequencing, RAD-seq and SNP array genotypes are available. We inferred ROH and individual inbreeding to evaluate the relative effects of sequencing depth versus SNP density on estimating inbreeding coefficients and found that high rates of missingness downwardly bias both the number and length of ROH. In summary, when using genomic data to evaluate inbreeding, studies must consider that ROH estimates are heavily dependent on analysis parameters, dataset density and individual sequencing depth.

Keywords: *whole-genome resequencing*; *genomic inbreeding*; *runs of homozygosity*; *SNP array*; *conservation genomics*; *Notiomystis cincta*

1. Introduction

Mating between close relatives may reduce fitness in offspring, an effect attributed to the unmasking of deleterious recessive mutations in regions of the genome that are rendered identical by descent (IBD; Charlesworth & Charlesworth, 1987; Bosse et al., 2019). Whilst inbreeding is generally undesirable, the stakes are especially high in at-risk species, for example where genetic diversity has been reduced by severe bottlenecks or habitat fragmentation (Maya-Garcia et al., 2017). For these reasons, estimation of the inbreeding coefficient (F) is commonly used in ecology, evolution and conservation biology where it may be employed as a proxy for adaptive potential and to inform population management strategies (Hoffmann et al., 2017).

Early attempts to quantify inbreeding relied solely on pedigree-based estimators (F_{PED}; Kardos et al., 2016) until the widespread adoption of microsatellite markers in molecular ecology. Multi-locus microsatellite genotypes were frequently incorporated to validate and add to observational pedigrees (Pemberton, 2008) or to estimate multi-locus heterozygosity (MLH; Coltman et al., 1999; Marshall & Spalton, 2000; Slate et al., 2000), which is expected to correlate with inbreeding if there is high variance in inbreeding in a population (Slate et al., 2004). As genomics technologies have advanced, genome-wide data is increasingly being employed to generate large datasets of single nucleotide polymorphisms (SNPs) that can be used to estimate MLH or genomic inbreeding coefficients (Leutenegger et al., 2003; Huisman et al., 2016b; Zilko et al., 2020).

In addition to the genome-wide inbreeding measures, it is possible to determine the distribution and size of regions of the genome that contain runs of homozygosity (ROH). The idea of using runs of homozygosity as a means of understanding inbreeding has its origin in human studies (Broman & Weber, 1999; Gibson et al., 2006; McQuillan et al., 2008), but has been widely embraced in the agricultural and horticultural communities (Sölkner et al., 2010). To-date, most ROH-based studies have come from primary industry, particularly commercial livestock breeding (e.g. cattle in Zhang et al., 2015 and in Forutan et al., 2018; horses in Grilz-Seger et al., 2018; pigs in Bosse et al., 2012; Schiavo et al., 2020). Quantifying ROH on a large scale, sometimes involving hundreds of thousands of individuals, has proved a useful tool to track an individual's ancestry (Kirin et al., 2010), find and explain variation

across individuals and populations (Pemberton et al., 2012) and to better understand their demographic history and disease architecture (Ceballos et al., 2018b). Longer stretches of homozygous segments are assumed to reflect IBD through recent inbreeding, whereas shorter runs indicate a more historic inbreeding event (Curik et al., 2014). Very short ROH are typically excluded from any inbreeding analysis, as they could simply occur due to population-specific linkage disequilibrium between markers (Ferenčaković et al., 2013; Pryce et al., 2014). To estimate genome-wide inbreeding F_{ROH}, the total sum of all runs of homozygosity segments is divided by the size of the autosomal genome of a species.

Relatively little research on ROH has been performed in non-model organisms. However, a key insight from ROH studies has been that a large proportion of deleterious homozygous genotypes seem to fall into ROH (Szpiech et al., 2013), leading to the prediction that ROH detection could be one of the most powerful methods to investigate inbreeding depression (Keller et al., 2011). As genomic technologies have become more affordable, the opportunity to infer individual ROH in animals of high ecological importance or of conservation concern has therefore received increasing attention (Grossen et al., 2018; Hooper et al., 2020; Humble et al., 2020; Wang et al., 2021; Escoda & Castresana, in press). For example, a large-scale collared flycatcher (*Ficedula albicollis*) study on genomic inbreeding and historical demography found ROH sizes between 953bp and 17.5Mbp (Kardos et al., 2017), with highest ROH abundance in regions of low recombination rate. Moreover, population-level studies of Isle Royale wolves (*Canis lupus*) revealed high variance in genomic inbreeding between individuals, with some individuals showing homozygosity across whole chromosomes (Hedrick et al., 2017; Kardos et al., 2017).

SNP datasets can be generated at resolutions ranging from whole genome resequencing, to reduced representation approaches, such as restriction site-associated DNA sequencing (RAD-seq), and targeted SNP genotyping, for example using SNP arrays. In agricultural applications, SNP arrays harbouring between 50,000 (e.g. sheep (*Ovis aries*) in Purfield et al., 2017) and 200,000 (e.g. coho salmon (*Oncorhynchus kisutch*) in Yoshida et al., 2020) high quality, informative markers across the genome are commonly employed to estimate inbreeding. Although SNP arrays have also been applied to estimate inbreeding in wild populations in a handful of cases (Huisman et al., 2016a; Vendrami et al., 2019), genome-wide SNP datasets to estimate inbreeding in ecology and evolution are generated

primarily from reduced representation and whole-genome resequencing approaches (Hoffman et al., 2014; Knief et al., 2015; Berenos et al., 2016; Kardos et al., 2018a; Robinson et al., 2019; Niskanen et al., 2020). Compared to SNP arrays, these datasets differ in the density of genotyped sites and in the confidence of genotype calls, as well as their scalability and their costs (Davey et al., 2013; Fuentes-Pardo & Ruzzante, 2017).

The accuracy of inbreeding measures in a population is dependent on linkage disequilibrium between neighbouring markers, which is influenced by factors such as the effective population size and selection intensity (Ceballos et al., 2018b). We therefore assume that larger SNP datasets are better at capturing a 'true' inbreeding value (Hillestad et al., 2017), however, the high costs of high coverage whole-genome resequencing across many individuals makes this approach unfeasible for most wild populations (Minias et al., 2019). As low-coverage whole-genome resequencing data is less costly to generate, it could prove to be a promising alternative to SNP array datasets if genotyping many more loci outweighs the risk of underestimating heterozygous calls due to low per-site depth, leading to ROHs being overestimated (Ceballos et al., 2018a). Conversely, for both SNP array and sequencing data, there is also the possibility that some genotypes are miscalled as heterozygyote, which may underestimate some ROHs. In addition, for both low coverage resequencing and for reduced representation approaches, the uneven distribution of genotyped markers across the genome may mean that certain regions of the genome are overlooked and some ROH remain undetected. Further, a recent review examining dozens of ROH studies (Meyermans et al., 2020) has found that many studies lack an explanation for why certain software parameters to detect ROH were chosen and fail to examine what impact that could have based on the marker density or sequencing depth of a given dataset (e.g. failing to detect ROH, or screening only parts of the genome).

In species conservation, it is essential to be able to draw reliable conclusions about the level of consanguinity between individuals. This is especially important if populations are small, natural dispersal is limited and individuals chosen for breeding programs and translocations originate from the same remnant source population (Weeks et al., 2011; Armstrong et al., 2021). Maintaining a healthy level of genetic diversity is important in conservation management, but obtaining accurate knowledge of this diversity can be difficult and expensive to obtain from large-scale population genomics analysis. Hence,

with the growing number of low coverage and reduced representation resequencing studies (Puckett, 2017), it is important to address what influence marker density and marker type has on evaluating identity-by-decent. This will help to correctly infer the conservation status and adaptive potential of a species (McMahon et al., 2014; Hedrick & Garcia-Dorado, 2016; Kardos et al., 2016; McLennan et al., 2019; Alemu et al., 2021).

In this manuscript, we explore and evaluate the impact of different genotype datasets on estimating inbreeding in the hihi (*Notiomystis cincta*; stitchbird), an endemic, Vulnerable passerine bird of Aotearoa New Zealand. Genome-wide genotype datasets have been obtained using a custom 50K SNP array, RAD-seq and low-coverage whole genome resequencing. In conjunction with a draft hihi reference genome, this data allows us to assess how the properties of these different SNP datasets can influence our assessment of inbreeding in a model system for conservation genomics.

2. Materials and Methods

Study system and sampling

The hihi is an endemic Aotearoa bird that was once distributed across Te Ika a Māui (the North Island). Deforestation and the introduction of predatory mammals led to a sharp decline in hihi numbers, until by the 1880s only one population on Te Hauturu-o-Toi (Little Barrier Island; 36°12'S, 175°05'E), in the Hauraki Gulf, remained (Brekke et al., 2011). Today, re-established populations of hihi can be found in seven different mammalian predator-free sanctuaries, including on the island of Tiritiri Matangi (36°36'S, 174°53'E). This study includes data for three hihi nestlings from Tiritiri Matangi, sampled in the 2012/2013 austral breeding season, and one adult sampled on Te Hauturu-o-Toi in 2006/2007, six adults in 2010/2011 and one adult male sampled in October 2017. The blood sample from the 2017 Te Hauturu-o-Toi male has been utilised to assemble a high quality reference genome while the other ten samples have been genotyped with low coverage whole genome resequencing (4.2-9.8x), RAD-seq and a SNP array (see below). We refer to the genome assembly individual as *Yellow* in reference to the vibrant *Yellow* neck and shoulder feather band found on hihi males. The remaining ten birds are labelled as *Hihi_01 - Hihi_10* and were selected to represent both the historic population and the largest of the

reintroduced populations, which have current population sizes of around 2,000 and 200 hihi respectively (Parlato et al., 2021).

Genome assembly for the reference individual

We generated a draft genome assembly for *Yellow* using Oxford Nanopore Technologies (ONT) long read sequencing. Genomic DNA was extracted using the NEB Monarch gDNA extraction. Sequencing libraries were prepared using the ligation sequencing kit (LSK-109) and run across 8 MinION R9.4.1 flow cells. To maximise output, flow cells were flushed with the nuclease wash kit (WSH-003) and new library loaded 3-5 times during each sequencing run. A total of 62.7 Gb raw data was obtained following base-calling with Guppy v3.6.2 (https://github.com/nanoporetech). This data was filtered to remove any contaminating adaptor sequence using PoreChop v0.2.4 (Wick et al., 2017). Further filtering was performed with NanoPack tools (Wick et al., 2017): sequences derived from the DCS internal control were removed with Nanolyse v.1.2.0; reads were also filtered for quality (>q10) and to exclude reads shorter than 5 kb using NanoFilt v 2.6.0.

The filtered dataset of 42.22 Gb with a read N50 of 14.8 kb was assembled using FLYE v2.7 (Kolmogorov et al., 2019) with the "keep haplotypes" flag enabled. The same reads were then used for two rounds of assembly polishing with racon (v 1.4.13). The resulting draft assembly has a total size of 1,058.9 Mb and is comprised of 1,117 contigs, with a contig N50 of 6.768 Mb. 98.2% of the assembly sequence is contained in 260 contigs of 300kb or greater. Genome completeness is 92.2% as measured using BUSCO v 4.1.4 (Simao et al., 2015) with the odb10_aves dataset.

The assembly was repeat masked using Repeat Masker v4.1.0 (Smit et al., 2015a) with a custom library created by combining all known avian repeats from Dfam release 3.2 (Hubley et al., 2016) with the output of *de novo* repeat identification in the draft hihi genome using RepeatModeler (open-1.0.11; Smit et al., 2015b). In total, 146.7 Mb, corresponding to 13.86% of the genome, was excluded by masking.

Genomic data and SNP genotyping

All ten additional hihi under investigation have RAD-seq data, whole genome resequencing, and have been genotyped using a custom 50K Affymetrix SNP array. This array was developed before the

generation of the hihi reference genome through identification of SNPs from *de-novo* assembly of RAD-seq from 26 individuals, including these ten birds, and low-coverage whole-genome sequencing (lcWGS) of these ten individuals (detailed in de Villemereuil et al. (2019), Duntsch et al. (2020) and Lee et al. (*in prep*)). Of the 58,466 SNPs included on the array, 45,553 markers passed initial default quality control metrics in the Axiom Analysis Suite software and were classified as 'PolyHighResolution' (i.e., polymorphic SNPs with call rate of >95%, at least two minor alleles observed and genotype clusters well-separated) and were used in these analyses.

To locate SNPs from the lcWGS, RAD-seq and SNP array datasets in the reference assembly we mapped these datasets onto the assembly contigs. SNPs included in the SNP array were localised to positions in the *Yellow* reference assembly by BLAST searches using flanking sequences. The RAD-seq data from the ten individuals was processed through the Stacks 2.53 pipeline (Catchen et al., 2013). Raw reads were submitted to process_radtags with default parameters. Individual, filtered read sets were mapped to the *Yellow* reference assembly using BWA-mem v0.7.17 (Li, 2013), manipulated in SAMtools v1.10 (Li et al., 2009) and then run through the Stacks populations analysis module as a single population to call SNPs. The lcWGS dataset reads were first quality-filtered using Trimmomatic (v0.39; Bolger et al., 2014) with default settings and then aligned to the reference using BWA-mem. Genotyping was performed with GATK Haplotype Caller (v4.1.4.1) in GCVF mode (with -ERC BP_RESOLUTION; Poplin et al., 2018). Both the RAD-seq and lcWGS SNP datasets were filtered with *BCFtools 1.10.2* to include only biallelic sites with a minimum minor allele count of three and SNPs in repeat regions excluded. In addition, the lcWGS dataset was filtered in *PLINK* v1.9 (--max-missing 0.8 --maf 0.02; Chang et al., 2015) to ensure low levels of genotype call missingness. As recommended in Meyermans et al. (2020), no pruning for minor allele frequency or linkage disequilibrium was performed on any of the medium-density genotype datasets (RAD-seq, SNP array data). The RAD-seq data contains 26,447 SNPs with 18% average missing data, while the lcWGS filtering resulted in a final dataset containing 2,018,863 genomic markers with a mean coverage of 7.45 and 2.2% missing data (Supplementary Table S1).

To explore datasets of different marker density and quality, the lcWGS data for all ten hihi was divided into marker sets at five different call depth stringency levels. In the first instance, the data remained as

it was (2,018,863 sites; henceforth "lcWGS"), and in four other cases we adjusted the minimum mean depth (--min-meanDP) filtering threshold value in *vcftools* (Danecek et al., 2011). Only sites with mean depth values of greater than or equal to 6, 7, 8 and 9 over all ten individuals are included in those new datasets, leaving 1,746,437 ("lcWGS6"), 1,302,507 ("lcWGS7"), 644,631 ("lcWGS8") and 195,184 ("lcWGS9") variants for further analysis.

SNP genotyping for the reference individual

Genotype calls for *Yellow* were obtained by mapping the long reads back to the reference assembly using Minimap2 v2.17 (Li, 2018) and calling sequence variants using longshot v0.4.1 (Edge & Bansal, 2019). The list of variant sites identified in a first round of genotyping were then augmented by sites identified as variable in the other sequence/genotyping datasets from the ten individuals and recalled. Genotypes were called at the mapped lcWGS, SNP array and RAD-seq SNPs, as well as one dataset combining all variants (including unique variants detected only in the reference genome assembly), for sites in the reference genome that had a longshot genotype quality (GQ) of greater than 150. These datasets comprise 1,562,384 (lcWGS), 46,136 (SNP array) and 18,415 (RAD-seq) sites, with 1,593,073 total variants when combining across datasets (combined; information on inter-marker distance for each dataset in Supplementary Figure S1 and on frequency distribution in Supplementary Figure S2). Note that the total number of SNP array and RAD-seq sites genotyped in *Yellow* is slightly lower than for the set of ten individuals, as some SNP sites did not meet the base quality threshold in the reference male.

Finally, a "whole genome" dataset was constructed with 904,228,112 sites, providing sufficient resolution to estimate the "true" inbreeding value for this reference individual. To do so, we extracted genotype calls from the assembly where possible (where homozygous calls GQ>100 and heterozygous calls GQ>150) and assumed all other sites reaching a base quality of >100 and depth threshold of ten were homozygous. Sites were excluded if they were annotated as repeats or fell in regions with >2 SNPs in a 100bp window (assessed from the combined SNP dataset). To acquire additional datasets of different SNP densities, the combined dataset of 1,593,073 SNPs was then randomly down-sampled to subsets of SNPs representing 1/2 (*i.e.*, 796,537 SNPs), 1/4, 1/8, 1/16, 1/32, 1/64, 1/128 and 1/256 (*i.e.*, 6,223 SNPs) of the total, with ten replicates for each. In addition, ten replicate datasets sampling the number of SNP array and RAD-seq SNPs at random from the combined dataset were also generated.

Runs of homozygosity

ROH were first examined with the sliding windows approach in *PLINK* using the *--homozyg* function. Given the differences in the density of SNPs across the genome for each dataset, we followed the suggestion by Kardos et al. (2015) to tailor the settings for the ROH analysis with the aim to detect runs in a consistent manner across the SNP datasets. In particular, we adjusted the minimum average density of SNPs, the maximum gap length between adjacent SNPs, the size of the sliding window and the minimum number of variants needed to be able to detect a ROH to reflect the average SNP density of each dataset (Supplementary Methods; Supplementary Table S2). We allowed for one (for the SNP array and RAD-seq datasets) or two (for the higher density datasets) heterozygous and one missing site per window, to account for possible genotyping errors. In order to report comparable total lengths of homozygous segments across datasets, we set the required minimum length for ROH to 300kb, ensuring that short ROH deriving from linkage disequilibrium are excluded (Meyermans et al., 2020). These adjusted *PLINK* settings were applied to infer runs of homozygosity for both the reference genome individual (*Yellow*) and for the additional ten birds (*Hihi_01 - Hihi_10*). Detailed explanations about how the chosen settings were optimised can be found in the Supplementary Methods. We calculated the genome coverage parameter (the maximal ROH length the analysis can discover) of our SNP datasets by converting all SNPs in the different datasets to homozygous, determining the total inferred size of homozygous regions >300kb, and dividing this number by the total assembled genome size of 1,046.4 Mb (Meyermans et al., 2020).

For *Yellow*, we assessed the concordance between the full genome and each of the other datasets by subsampling the full genome to the SNPs shared with the focal dataset and calculating (i) the proportion of SNPs called within a ROH in the full genome that were also called within a ROH in the focal dataset and (ii) the proportion of SNPs called outside a ROH in the full genome that were also called outside a ROH in the focal dataset.

Inbreeding coefficients and multi-locus heterozygosity

Individual inbreeding coefficients based on detected runs of homozygosity (F_{ROH}) were estimated by summing the length of all ROH greater than 300kb and 500kb and dividing the sum by the assembly size of contigs >300kb (1.04 Gb) and >500kb (1.035 Gb).

Furthermore, for the ten individuals for the lcWGS, SNP array and RAD-seq datasets, genomic inbreeding coefficients F_G were calculated using *PLINK*. *PLINK* implements the --ibc function from the software GCTA (Yang et al., 2011) to report three measures of F_G, we here report method III, which is based on the correlation between uniting gametes (F_{IBC}). *PLINK*'s --het function was also used to calculate F_G based on observed autosomal homozygous genotype counts for each individual (F_{HET}).

MLH was inferred with the lcWGS8 dataset using the *InbreedR* (Stoffel et al., 2016) package in R (R Core Team, 2013). Correlation coefficients between MLH and all genomic inbreeding estimates for the ten hihi were calculated using Pearson statistics in R.

In addition, we scanned the datasets for the ten hihi (*Hihi_01 - Hihi_*10) for homozygous-by-descent (HBD) segments (Druet & Gautier, 2017) using the R package *RZooRoH* (Bertrand et al., 2019). *RZooRoH* implements a hidden Markov model to identify HBD segments and allows for the estimation of an inbreeding coefficient $F_{RZooRoH}$. The genotyping error rate was set to 0.25% (Ferenčaković et al., 2013). The analysis was performed using a mixKR model, with K = 4, 8 and 13 as the number of age-related HBD classes. Following advice from an *RZooRoH* author, inbreeding over all classes for K = 4 (Tom Druet, *pers comm*) was summed and correlated with *PLINK* ROH-based inbreeding estimates across all ten hihi individuals (as seen in Meyermans et al., 2020).

All summary statistics, correlations, and plots were generated in R using the R packages *ggplot2*, *dplyr*, *ggpubr*, *data.table* and the bird colour-based package *Manu*.

3. Results

Runs of homozygosity: *Yellow*, assembly bird

The number and length of runs of homozygosity found across the *Yellow* genome were relatively consistent across the different genotype datasets. The full genome dataset detected 270 ROH of >300

kb with a total length of 210,000 kb and an average length of 750 kb, and a realised F_{ROH} ($\geq$ 500 kb) of 0.15. Comparing these "true" estimates to the number and length of ROHs and the inbreeding values from the other datasets suggests that the SNP array data is slightly overestimating individual inbreeding, while the lower genotype density RAD-seq panel yields slightly lower values than expected (Table 1; Supplementary Table S3). The genome coverage parameter for the different datasets ranged from 54% for the RAD-seq data, to 93% for SNP array data, to 98% for the WGS and combined genome data.

Table 1: Output from the ROH analysis in PLINK for the assembly male Yellow. Each dataset has been scanned for runs of homozygosity ≥300kb using custom parameters depending on SNP density. Displayed are: the total number of genotyped sites, the genome coverage parameter, the number of these sites detected within an ROH, the percentage of SNPs that are also in a run when scanning the full genome, the percentage of SNPs that are also outside a ROH when scanning the full genome, the total number of ROH found, the total length of all ROH in kb, inbreeding (F_{ROH}) estimated as the total length of detected runs divided by the sum of contigs larger than the minimum ROH size of 300kb and F_{ROH} when considering ROHs of ≥500kb. Detailed PLINK ROH settings in Supplementary Methods and Supplementary Tables S2 and S3.

	Full genome	Combined	WGS	SNP array	RAD-seq
Genotyped sites	904,228,112	1,593,073	1,562,384	46,136	18,415
Genome coverage parameter		98.3%	98.3%	93.4%	54.2%
#sites in ROH	176,447,917	263,068	290,384	11,421	6,021
% agreement with full genome on ROH exclusion		96.0%	97.1%	81.0%	62.7%
% agreement with full genome on ROH inclusion		95.9%	95.4%	88.1%	72.5%
Total # of ROH	270	290	300	223	285
Total length (kb)	201,000	199,335	207,481	236,390	186,613
F_{ROH} ($\geq$ 300kb)	0.202	0.192	0.199	0.227	0.179

F_{ROH} (≥ 500kb)	0.149	0.138	0.144	0.224	0.130

When subsetting the full genome SNPs to only those SNPs found in the smaller datasets, 96% of the SNPs within a ROH for the full genome are also in a run for the combined dataset, and 97% for the WGS dataset (Table 1). Despite a relatively low SNP density, the SNP array data successfully called 81% of true ROH, and correctly identified 88% of regions that did not contain a ROH. While performing similarly overall in terms of the true number and length of ROHs, the RAD-seq data showed less overlap of ROH (63%) and non-ROH regions (73%). Lower density datasets may miss, underestimate or overestimate the length of ROHs (Figure 1).
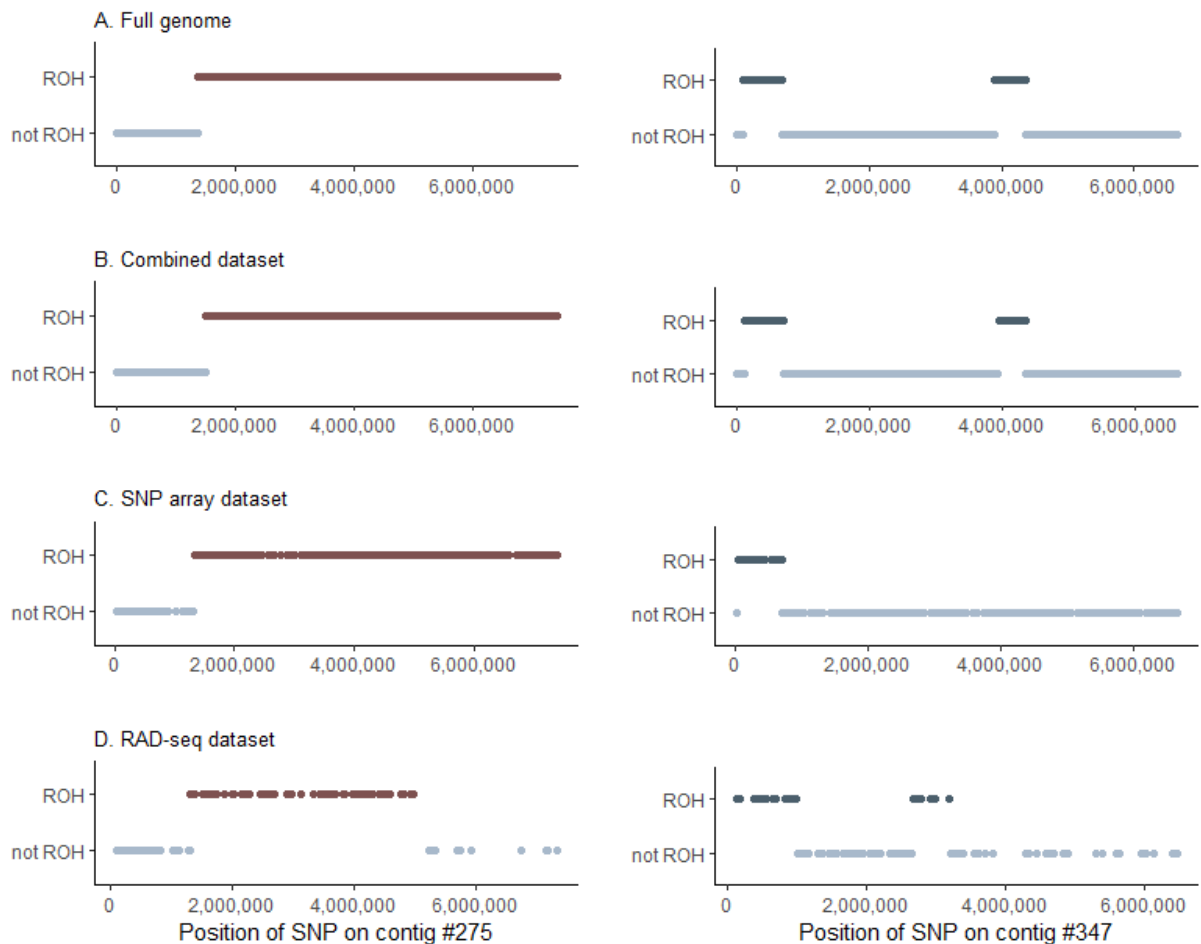
Figure 1: Two example contigs (#275 and #347) showing the detection of runs of homozygosity for the genome individual Yellow *using different marker densities. Positions in light blue were not involved in a ROH, while positions in dark red (#275) and dark blue (#347) were. For each contig, (A) denotes full genome sequence, (B) denotes the combined SNP dataset based on heterozygote calls in the dataset, and inferred genotypes at lcWGS, SNP-array and RAD-seq positions, (C) denotes inferred SNP-array genotypes, (D) denotes inferred RAD-seq genotypes.*

Down-sampling the combined *Yellow* dataset revealed that the RAD-seq and SNP array data behave somewhat differently from a dataset with the same number of SNPs sampled randomly across the genome (Figure 2), which may reflect a non-random distribution of these datasets across the genome and differences in the SNP minor allele frequency distributions for the different datasets (Supplementary Figure S1, S2). For *Yellow*, all down-sampled datasets with more than 100,000 variants yielded a total number and length of ROH, and hence an inbreeding value F_{ROH}, close to the full genome inbreeding level, while also maintaining high levels of concordance in terms of regions detected as inside or outside a ROH (Figure 1, Figure 2). The lower-density data also performed reasonably well compared to our gold standard full genome sequence, although datasets of <25,000 SNPs showed considerable declines in the number and accuracy of ROH calls (Figure 2).

Figure 2: The number and total length of ROH found, the percentage of SNPs that are also in a run when scanning the combined dataset (% agreement on inclusion) and the percentage of SNPs that are also outside a ROH when scanning the combined dataset (% agreement on exclusion), when randomly down-sampling the combined dataset that was generated for the male hihi. The number of variants are displayed on a log scale. The array and RAD-seq densities were i) generated via random down-sampling to the same total number (grey dots) but also ii) displayed with real RAD-seq and SNP array positions (the latter labelled in red). Note that the high % agreement on exclusion for the two smallest datasets are due to these datasets detecting very few ROHs; these failures to detect ROHs are reflected in the low % agreement on inclusion. The trend line was plotted with the geom_smooth(method = "loess") function in ggplot2 in R. Detailed PLINK ROH settings in Supplementary Material and Supplementary Tables S2-S5.

Runs of homozygosity: ten sampled hihi

For the ten hihi, the level of per-bird genotype missingness of the resequencing and the RAD-seq datasets was a major determinant of the ability to detect ROHs using *PLINK*. The number of ROH detected and the total length of ROH were negatively correlated with the initial missingness in all lcWGS datasets, although the relationship was relatively weak when correlating initial missingness against the

number and total length of ROHs for the lcWGS9 dataset (R = 0.275 and -0.304 respectively, Supplementary Tables S5 and S6). The RAD-seq ROH numbers and lengths were strongly negatively correlated with SNP missingness (R of -0.982 and -0.984 respectively) and were poorly correlated with all other ROH measures from the SNP array and lcWGS datasets (Supplementary Table S6). Excluding the two individuals with the lowest number of RAD-seq reads (<4 million) reduced the correlation with missingness somewhat, but negative correlations were still strong (R of -0.773 and -0.805 for ROH number and length respectively).

The total length of ROH detected from the high-confidence lcWGS9 dataset ranged from 173,564 to 255,175 kb, with a similar range of total ROH lengths in the SNP array dataset and in the lcWGS8 dataset once the two lowest coverage individuals were excluded. Total ROH lengths were similar to the lcWGS7 and lcWGS6 datasets when the three lowest coverage individuals were excluded, and in the lcWGS dataset when the four lowest coverage individuals were excluded (Supplementary Table S5). The inconsistency of ROH lengths in the lowest coverage individuals suggests that the *PLINK* ROH parameters based on average SNP density across individuals are unlikely to be optimal for individuals with high levels of missing data. A similar pattern is evident for the *RZooRoH* method, where the data with higher genotype missingness (RAD-seq) seems to overestimate the proportion of homozygous segments belonging to higher HBD classes (Supplementary Table S9).

The detailed display of contig 436 (Figure 3, Supplementary Figure S3) demonstrates that while *PLINK* analysis of RAD-seq data, SNP array data and lcWGS data is able to detect runs of homozygosity across individuals, these runs may not be consistent. On the figure, higher peaks indicate that this region is shared as a ROH across a larger proportion of individuals. Regions that are homozygous across many individuals appear in the centre of the runs, while as segments move closer to the edge of a ROH, fewer individuals are involved in it (*i.e.*, an A-shape). For this contig, no SNP is present within a ROH for all individuals in any of the datasets.

Whether the ROH patterns and lengths agree with each other, however, is dependent on whether the initial dataset SNP density is high enough for that specific contig and for each individual. Generally, the lcWGS datasets perform similarly with the higher quality (higher average mean coverage) data showing more pronounced and comparable ROH patterns than the raw, unfiltered lcWGS dataset

(Supplementary Figure S3). For contig 436, the SNP array data generally agrees with the lcWGS8 landscape, but peaks are broader. The RAD-seq data also detects runs, but partly in areas were the other datasets are clearly heterozygous, and appears to miss ROHs due to particularly low SNP density in some regions, in agreement with results from down-sampling the whole genome individual *Yellow* (Table 1, Figure 1). Inference of ROHs using *RZooRoH* shows similar inconsistencies across different datasets (Supplementary Figure S4).
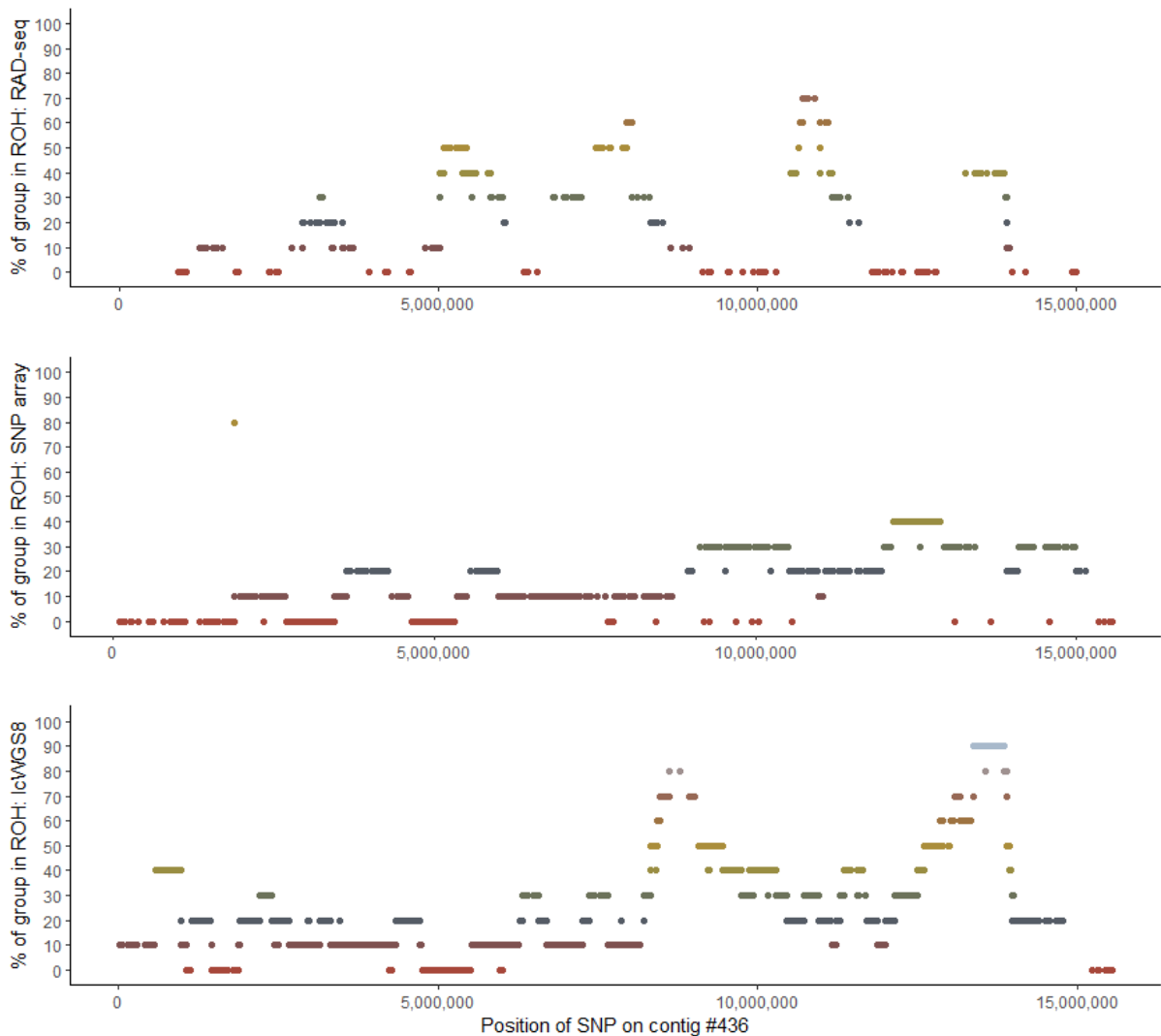
Figure 3: Location of runs of homozygosity (ROH) for one example contig (#436) that had ROH detected across all seven datasets, with ROH landscapes shown for the RAD-seq, SNP array and lcWGS8 datasets. Displayed are the percentage of the ten birds (y-axis) that have this SNP (x-axis) involved in a run of homozygosity. The more individuals share the ROH, the higher the SNP is located in the plot. Red dots at the bottom of the plot mean that those SNPs were not involved in a ROH in any bird. ROH for the other datasets shown in Supplementary Figure S3, SNPs in HBD segments according to RZooRoH shown in Supplementary Figure S4.

For these ten hihi, the landscape of *PLINK* runs of homozygosity differed between contigs, with some contigs portraying a similar picture across datasets, while others yielded completely different numbers and lengths of ROH (contig sizes and the number and length of ROHs detected for each individual are shown in Supplementary Table S7). Similarly, *RZooRoH* homozygosity landscapes for the different datasets had little concordance with each other, as highlighted in an example contig (Supplementary Figure S4). As noted, given that inter-marker distances differ along the genome, ROHs in certain regions are likely to be undetectable in some of the datasets (Meyermans et al., 2020), as is apparent for the RAD-seq data for the majority of contigs. The number of contigs that were consistently involved in at least one run of homozygosity across all datasets was 87, with an additional 102 across all datasets excluding the RAD-seq output.

Inbreeding coefficients and MLH

With our chosen parameter settings in *PLINK*, we detected comparable levels of inbreeding F_{ROH} in *Yellow* and the ten additional hihi. Similar to the ROH analyses, the ROH-based individual inbreeding estimates for the ten hihi were sensitive to the amount of missing data in the lcWGS and RAD-seq datasets: individuals with high rates of missing data yielded much lower whole-genome inbreeding estimates. After excluding low-coverage individuals, the SNP array and RAD-seq datasets show good agreement with the lcWGS datasets results for F_{ROH} (Supplementary Table S8). Based on F_{ROH} from lcWGS data, individuals *Hihi_05* and *Hihi_09* appear most inbred in the dataset and we detect slightly higher average inbreeding levels in Tiritiri Matangi birds than in Te-Hauturu-o-Toi individuals (0.16 vs 0.11; using lcWGS8 data).

In addition to F_{ROH}, the inbreeding measures $F_{RZooRoH}$, F_{IBC} and F_{HET} were calculated for the ten hihi (Supplementary Table S8/S9). $F_{RZooRoH}$ estimates for the ten hihi were more consistent across all WGS coverage levels than F_{ROH} measures, but equally sensitive to the high levels of genotype missingness in the RAD-seq datasets. While the model-based *RZooRoH* approach yielded higher inbreeding values than *PLINK* (as seen in Meyermans et al., 2020) the inbreeding values per individual were highly correlated for almost all datasets between the two approaches (R = 0.80-0.94; Supplementary Table S9; Supplementary Figure S5).

After excluding the low coverage individuals, the high confidence lcWGS8 dataset showed very strong ($R > 0.94$) correlations between F_{ROH} and $F_{RZooRoH}$, and between F_{IBC} and F_{HET}. F_{IBC} and F_{HET} were also strongly correlated with MLH. The ROH- based inbreeding estimates were also well correlated ($R = 0.58$ - 0.72) with the marker-based genomic estimates F_{IBC} and F_{HET} and with MLH. Detailed correlations across datasets and methods can be found in Supplementary Tables S8, S9, S11 and S12 and Supplementary Figures S5 and S6. The lcWGS datasets with a mean per-site depth of eight and nine show the highest correlation and the most robust results across individuals and methods to calculate F from ROH-based inbreeding estimates.

4. Discussion

Here we incorporate RAD-seq, SNP array and whole-genome resequencing data of different resolutions into a population genomics study to evaluate the methods for estimating inbreeding in an animal species of conservation concern. We find that low density datasets may miss ROH due to large gaps between called sites, but can also combine two shorter homozygous regions together and inflate ROH length. In addition, we find that very low-coverage resequencing data (4-6x) may be unreliable and these low depth sites (potentially incorrectly called as homozygous) should be removed from the dataset prior to any analysis. Our results suggest a trade-off in low coverage data, where the landscape of ROH in any individual is dependent on the balance between SNP density and genotype call quality.

Estimates of ROH and inbreeding in hihi - which method works best?

For our whole-genome hihi from Te Hauturu-o-Toi, the ROH inbreeding analysis based on segments larger than 500 kb yielded a similar inbreeding coefficient across all datasets of various marker densities, suggesting a relatively high genomic inbreeding level of 0.15. Inbreeding levels of the additional ten hihi individuals are concordant with this measure, with F_{ROH} values ranging from 0.12 to 0.20 based on the lcWGS9 data, slightly higher than previous microsatellite-based hihi inbreeding measures (Brekke et al., 2010). Our hihi inbreeding levels are higher than F_{ROH} in the more abundant collared flycatchers (Kardos et al., 2017) but similar to estimates for low-population size species such as the critically endangered helmeted honeyeater *Lichenostomus melanops cassidix* (Harrisson et al., 2019) or the crested ibis

(*Nipponia nippon*; 0.19-0.32, Li et al., 2014). Similar to hihi, the ibis also underwent a recent bottleneck, but we note that *PLINK*'s ROH-based inbreeding estimates are sensitive to the parameter settings chosen and hence comparing inbreeding values across species warrants caution.

For hihi, we find that conclusions from a model-based approach implemented by *RZooRoH* are concordant with rule-based approach in *PLINK*, namely that the number and total size of ROH are sensitive to genotype missingness, the density of genotyped SNPs and the software parameter choices. Compared to *PLINK*, *RZooRoH* results appeared slightly more robust to low resequencing coverage.

After excluding individuals with low coverage, our inbreeding measures F_{ROH} and $F_{RZooRoH}$ were strongly correlated with each other, a finding similar to an evaluation on different livestock and pet species (Meyermans et al., 2020), and F_{ROH} and F_{IBC} were strongly correlated for the SNP array data. The slight differences in these estimates capture different aspects of inbreeding – for example, by giving greater weight to rare alleles, F_{IBC} is generally seen as one of the more accurate estimators of inbreeding (Keller et al., 2011; Chen et al., 2016). It is also likely to capture more distant inbreeding events than F_{ROH}, as F_{ROH} excludes short ROH (Pryce et al., 2014; Kardos et al., 2018b). However, within the context of conservation management, where inbreeding depression is of primary concern, F_{ROH} may offer the most appropriate measure (Kardos et al., 2018b). This is because in small populations with ongoing high levels of mating between relatives, it might be expected that purging has removed all but the most recent deleterious rare alleles (Caballero et al., 2017). The priority in these species of conservation concern is therefore to identify and assess individuals who are highly inbred due to very recent consanguinity, as these individuals are more likely to harbour two copies of recent deleterious rare alleles that have not yet been exposed to selection (Grossen et al., 2020; Stoffel et al., in press).

In addition to estimating inbreeding levels, *RZooRoH* is increasingly being used in order to investigate population history by adjusting K, with K-1 as the number of age-related HBD classes (Druet & Gautier, 2017): smaller K means longer HBD segments that reflect recent autozygosity, *i.e.*, a recent common ancestor. Both for *RZooRoH* and *PLINK*, higher density datasets offer the opportunity to detect smaller homozygous segments. In future, one could employ *RZooRoH* in order to calculate the physical lengths of the HBD segments found and compare their abundance to the size distribution of ROH runs estimated

in *PLINK* as well as perform more in-depth analyses of inbreeding levels across regions of the genome (Gorssen et al., 2020).

On the role of marker density and the importance of sufficient per-site depth

The main questions that motivated this paper were whether our conclusions about inbreeding in our eleven individuals would be different depending on the datasets employed, and whether the analysis strategy matters. The answers seem clear: the overall inbreeding values do not have to differ greatly if ROH settings are carefully chosen based on SNP density, but consistency in these overall inbreeding measures may hide differences in the ROH landscape between datasets.

By tailoring ROH-detection parameters to the SNP density of each dataset, we recovered consistent F_{ROH} individual inbreeding estimates from RAD-seq, low-coverage sequencing data and subsampled whole-genome sequence data. For all individuals the SNP array data slightly overestimated inbreeding, likely because the array SNPs were distributed less randomly across the genome and differed in their allele frequency distribution compared to a random dataset of the same size. However, the relative inbreeding across individuals was very consistent across RAD-seq, SNP chip and low-coverage resequencing datasets. It is a promising insight that relative inbreeding between individuals can be reliably estimated from low to medium density datasets. For the ten hihi from Tiritiri Matangi and Te Hauturu-o-Toi, the low-coverage whole-genome sequence data performed most consistently for individuals with higher average per-site depth. At lower average depth, the chance of incorrectly calling a heterozygote individual as a homozygote increases substantially (from 0.39% at depth 9, to 3.13% at depth 6, to 25% at depth 3). While there is the argument that more population genetic information can be drawn from studies involving larger sample sizes instead of focussing on per-site sequencing depth (Buerkle & Gompert, 2013), our work supports the conclusion that accurate individual-level inbreeding measures do require some filtering to ensure adequate read depth to be able to confidently call heterozygote sites (Fuentes-Pardo & Ruzzante, 2017).

Although overall inbreeding values are consistent, what is less clear for hihi is whether low-density marker sets are capturing the same runs, at the same locations, as would be captured by higher density data. For example, the relative consistency between RAD-seq and SNP array F_{ROH} with the full genome F_{ROH} appears to be partly due to the lower density datasets missing some ROHs completely and

overestimating the length of those that are detected. Indeed, only 63% of SNPs are called consistently as in a ROH when comparing full-genome and RAD-seq data, while the figure is 81% for SNP array data (Table 1). For species where a whole genome sequence assembly is available, we strongly encourage exploration of the detectability of true ROHs by subsampling SNP datasets to different levels, and reporting the concordance with the full genome, before designing a resequencing or genotyping strategy to estimate ROHs and overall inbreeding in a larger set of individuals.

In addition to dataset density, it is clear from the ten hihi with low coverage whole-genome data that, similar to F_{ROH}, the number and length of ROHs detected were heavily dependent on call missingness and sequencing depth. The two most consistent datasets in terms of ROH number and total lengths across individuals were the low coverage whole genome sequencing datasets where an average depth of eight (lcWGS8) or nine (lcWGS9) reads was required. Our results strongly suggest that low coverage individuals and sites should be excluded in order to reduce the risk of miscalling poorly genotyped regions as 'true' ROHs.

In the genome individual *Yellow*, fewer ROH of longer overall length were detected from the SNP array compared to the other SNP datasets. In addition, for the 10 birds, the SNP array ROH landscape across contigs often differed from the patterns observed from the low coverage sequencing datasets. Although there is still some scepticism around the use of SNP array data for ROH detection (Gladstein, 2018) and usage is still rare in a conservation context, numerous studies are employing medium-density SNP array data to detect ROH, especially in livestock species (Purfield et al., 2017). For existing marker sets, such as commercial or custom-made SNP arrays, we recommend that studies should routinely assess and report the genome coverage parameter to determine the detectability of true ROH. This will be especially important for species where LD is much lower and overall heterozygosity much higher than for our threatened hihi.

Accurate inference of ROH requires a marker dataset that is dense enough such that neighbouring markers are in LD with each other, and are informative about the unsampled sites between them (Karimi et al., 2020). Linkage disequilibrium is high in the species (Lee et al., *in prep*), perhaps unsurprising given the very low genetic diversity (de Villemereuil et al., 2019) and the known history of bottlenecks in hihi (Brekke et al. 2011). This suggests that fewer SNPs may be needed to accurately capture ROHs in hihi than for other, non-threatened species. In addition, our work has demonstrated that with appropriate

adjustments for marker density in the parameter settings when calling ROHs, datasets with as few as 25,000 SNPs in species with high LD, which includes many agricultural species, are able to accurately estimate both the number and total length of ROHs (Figure 2). Despite this, our hihi data also suggests that some RAD-seq datasets will indeed be too sparse to accurately infer ROH. Given the increasing availability of genome assemblies of a focal species (or close relative), we therefore strongly recommend mapping RAD-seq reads to the genome to estimate (i) the genome coverage parameter and (ii) whether ROHs are likely to be accurately inferred.

For population genomic studies dealing with a variety of dataset properties, we conclude that rather than imposing a minimum marker density, tailored ROH settings, adequate per-site depth and an understanding of the detectability of ROHs at different marker densities are the most important aspects required to draw meaningful conclusions about inbreeding levels based on ROH.

Why choosing the correct *PLINK* settings matters

PLINK is the most commonly used tool to find ROH, but there is little consensus on the optimal settings, even though most agree that the default is not suitable for most species (Gazal et al., 2014; Meyermans et al., 2020). We confirm this conclusion: when using default settings, the number and total size of ROHs detected decreased as the number of subsampled SNPs decreased (Supplementary Figure S7). While some manuscripts mention that adjusting most of the parameters is rather redundant (Hillestad et al., 2017), others reason that SNP density should be considered when scanning the genome for ROH (Ferenčaković et al., 2013). Some authors recommend allowing a certain level of heterozygous calls within a sliding window in order to account for genotyping errors, while others claim that allowing these will increase the number of false positive ROHs (Hillestad et al., 2017); our own data was relatively insensitive to the number of heterozygotes allowed within a window. A recent study simulating datasets of different resolutions and investigating them with different *PLINK* setting combinations, showed that for the smallest marker density the tool failed to detect any ROH (Shafer et al., 2016), which is in accordance with our hihi findings: even when tailoring settings to adjust for SNP density, a dataset of less than 20,000 SNPs yields significantly lower F and number of ROH (Figure 2). Above a required density to capture LD between adjacent SNPs, our data strongly supports the importance of tailoring parameter settings to suit the SNP density, in particular the minimum density of SNPs to call a ROH,

maximum gap size between adjacent SNPs, minimum number of SNPs required to call a ROH, and the sliding window size. Our results also suggest that adjusting parameters for the local density of SNPs as the genome is parsed would be a helpful addition to the *PLINK* settings, as suggested by Meyermans (et al., 2020) and Ferenčaković (et al., 2013).

The future of inbreeding estimation in conservation genomics

There are a growing number of studies of wild populations that make use of whole-genome resequencing data (Zhao et al., 2013; Xue et al., 2015; van der Valk et al., 2019). The rapidly falling costs of sequencing have enabled a remarkable explosion in the number of genome assemblies, and, along with growth in bioinformatics capacity within the field of conservation genetics, mean that resequencing is likely to become the go-to-method in conservation in the future (Narum et al., 2013). Our results suggest that, given appropriate choice of parameter combinations, and assessment of the marker density required to capture the linkage disequilibrium landscape, genomic estimates of inbreeding can offer considerable insight into the variation in individual inbreeding in a population. This will be of particular importance in addressing consequential conservation issues such as inbreeding depression (Kardos et al., 2016) and in assessing the genomic impact of management strategies such as captive breeding, reintroduction and assisted gene flow (Saremi et al., 2019).

Acknowledgements

References

Alemu, S. W., Kadri, N. K., Harland, C., Faux, P., Charlier, C., Caballero, A., & Druet, T. (2021). An evaluation of inbreeding measures using a whole-genome sequenced cattle pedigree. *Heredity, 126*(3), 410-423. doi:10.1038/s41437-020-00383-9

Armstrong, D. P., Parlato, E. H., Egli, B., Dimond, W. J., Kwikkel, R., Berggren, Å., . . . Ewen, J. G. (2021). Using long-term data for a reintroduced population to empirically estimate future consequences of inbreeding. *Conservation Biology, 35*(3), 859-869. doi:10.1111/cobi.13646

Berenos, C., Ellis, P. A., Pilkington, J. G., & Pemberton, J. M. (2016). Genomic analysis reveals depression due to both individual and maternal inbreeding in a free-living mammal population. *Molecular Ecology, 25*(13), 3152-3168. doi:10.1111/mec.13681

Bertrand, A. R., Kadri, N. K., Flori, L., Gautier, M., & Druet, T. (2019). RZooRoH: An R package to characterize individual genomic autozygosity and identify homozygous-by-descent segments. *Methods in Ecology and Evolution, 10*(6), 860-866. doi:10.1111/2041-210X.13167

Bolger, A. M., Lohse, M., & Usadel, B. (2014). Trimmomatic: a flexible trimmer for Illumina sequence data. *Bioinformatics, 30*(15), 2114-2120. doi:10.1093/bioinformatics/btu170

Bosse, M., Megens, H.-J., Madsen, O., Paudel, Y., Frantz, L. A. F., Schook, L. B., . . . Groenen, M. A. M. (2012). Regions of Homozygosity in the Porcine Genome: Consequence of Demography and the Recombination Landscape. *PLOS Genetics, 8*(11), e1003100. doi:10.1371/journal.pgen.1003100

Bosse, M., Megens, H. J., Derks, M. F. L., de Cara, A. M. R., & Groenen, M. A. M. (2019). Deleterious alleles in the context of domestication, inbreeding, and selection. *Evolutionary Applications, 12*(1), 6-17. doi:10.1111/eva.12691

Broman, K. W., & Weber, J. L. (1999). Long homozygous chromosomal segments in reference families from the centre d'Etude du polymorphisme humain. *The American Journal of Human Genetics, 65*(6), 1493-1500.

Caballero, A., Bravo, I., & Wang, J. (2017). Inbreeding load and purging: implications for the short-term survival and the conservation management of small populations. *Heredity, 118*(2), 177-185. doi:10.1038/hdy.2016.80

Catchen, J., Hohenlohe, P. A., Bassham, S., Amores, A., & Cresko, W. A. (2013). Stacks: an analysis tool set for population genomics. *Molecular Ecology, 22*(11), 3124-3140. doi:10.1111/mec.12354

Ceballos, F. C., Hazelhurst, S., & Ramsay, M. (2018a). Assessing runs of Homozygosity: a comparison of SNP Array and whole genome sequence low coverage data. *BMC Genomics, 19*(1), 106. doi:10.1186/s12864-018-4489-0

Ceballos, F. C., Joshi, P. K., Clark, D. W., Ramsay, M., & Wilson, J. F. (2018b). Runs of homozygosity: windows into population history and trait architecture. *Nature Reviews Genetics, 19*, 220-234. doi:10.1038/nrg.2017.109

Chang, C. C., Chow, C. C., Tellier, L. C., Vattikuti, S., Purcell, S. M., & Lee, J. J. (2015). Second-generation PLINK: rising to the challenge of larger and richer datasets. *GigaScience, 4*(1). doi:10.1186/s13742-015-0047-8

Charlesworth, D., & Charlesworth, B. (1987). Inbreeding depression and its evolutionary consequences. *Annual Review of Ecology and Systematics, 18*(1), 237-268. doi:10.1146/annurev.es.18.110187.001321

Chen, N., Cosgrove, E J., Bowman, R., Fitzpatrick, J W., & Clark, A G. (2016). Genomic Consequences of Population Decline in the Endangered Florida Scrub-Jay. *Current Biology, 26*(21), 2974-2979. doi:10.1016/j.cub.2016.08.062

Coltman, D. W., Pilkington, J. G., Smith, J. A., & Pemberton, J. M. (1999). Parasite-mediated selection against inbred Soay sheep in a free-living, island population. *Evolution, 53*(4), 1259-1267. doi:10.1111/j.1558-5646.1999.tb04538.x

Curik, I., Ferenčaković, M., & Solkner, J. (2014). Inbreeding and runs of homozygosity: A possible solution to an old problem. *Livestock Science, 166*, 26-34. doi:10.1016/j.livsci.2014.05.034

Danecek, P., Auton, A., Abecasis, G., Albers, C. A., Banks, E., DePristo, M. A., . . . 1000 Genomes Project Analysis Group. (2011). The variant call format and VCFtools. *Bioinformatics, 27*(15), 2156-2158. doi:10.1093/bioinformatics/btr330

Davey, J. W., Cezard, T., Fuentes-Utrilla, P., Eland, C., Gharbi, K., & Blaxter, M. L. (2013). Special features of RAD Sequencing data: implications for genotyping. *Molecular Ecology, 22*(11), 3151-3164. doi:10.1111/mec.12084

Druet, T., & Gautier, M. (2017). A model-based approach to characterize individual inbreeding at both global and local genomic scales. *Molecular Ecology, 26*(20), 5820-5841. doi:10.1111/mec.14324

Duntsch, L., Tomotani, B. M., de Villemereuil, P., Brekke, P., Lee, K. D., Ewen, J. G., & Santure, A. W. (2020). Polygenic basis for adaptive morphological variation in a threatened Aotearoa| New Zealand bird, the hihi (*Notiomystis cincta*). *Proceedings of the Royal Society B, 287*(1933), 20200948.

Edge, P., & Bansal, V. (2019). Longshot enables accurate variant calling in diploid genomes from single-molecule long read sequencing. *Nature Communications, 10*(1), 4660. doi:10.1038/s41467-019-12493-y

Escoda, L., & Castresana, J. (in press). The impact of bottlenecks and inbreeding on the genome of the endangered Pyrenean desman. *bioRxiv*, 2020.2007.2025.199281. doi:10.1101/2020.07.25.199281

Ferenčaković, M., Solkner, J., & Curik, I. (2013). Estimating autozygosity from high-throughput information: effects of SNP density and genotyping errors. *Genetics Selection Evolution, 45*(1), 42. doi:10.1186/1297-9686-45-42

Forutan, M., Ansari Mahyari, S., Baes, C., Melzer, N., Schenkel, F. S., & Sargolzaei, M. (2018). Inbreeding and runs of homozygosity before and after genomic selection in North American Holstein cattle. *BMC Genomics, 19*(1), 98. doi:10.1186/s12864-018-4453-z

Fuentes-Pardo, A. P., & Ruzzante, D. E. (2017). Whole-genome sequencing approaches for conservation biology: Advantages, limitations and practical recommendations. *Molecular Ecology, 26*(20), 5369-5406. doi:10.1111/mec.14264

Gazal, S., Sahbatou, M., Perdry, H., Letort, S., Génin, E., & Leutenegger, A. L. (2014). Inbreeding Coefficient Estimation with Dense SNP Data: Comparison of Strategies and Application to HapMap III. *Human Heredity, 77*(1-4), 49-62. doi:10.1159/000358224

Gibson, J., Morton, N. E., & Collins, A. J. H. m. g. (2006). Extended tracts of homozygosity in outbred human populations. *15*(5), 789-795.

Gorssen, W., Meyermans, R., Buys, N., & Janssens, S. (2020). SNP genotypes reveal breed substructure, selection signatures and highly inbred regions in Piétrain pigs. *Animal Genetics, 51*(1), 32-42. doi:10.1111/age.12888

Grilz-Seger, G., Mesaric, M., Cotman, M., Neuditschko, M., Druml, T., & Brem, G. (2018). Runs of Homozygosity and Population History of Three Horse Breeds With Small Population Size. *Journal of Equine Veterinary Science, 71*, 27-34. doi:10.1016/j.jevs.2018.09.004

Grossen, C., Biebach, I., Angelone-Alasaad, S., Keller, L. F., & Croll, D. (2018). Population genomics analyses of European ibex species show lower diversity and higher inbreeding in reintroduced populations. *Evolutionary Applications, 11*(2), 123-139. doi:10.1111/eva.12490

Grossen, C., Guillaume, F., Keller, L. F., & Croll, D. (2020). Purging of highly deleterious mutations through severe bottlenecks in Alpine ibex. *Nature Communications, 11*(1), 1001. doi:10.1038/s41467-020-14803-1

Harrisson, K. A., Magrath, M. J. L., Yen, J. D. L., Pavlova, A., Murray, N., Quin, B., . . . Sunnucks, P. (2019). Lifetime Fitness Costs of Inbreeding and Being Inbred in a Critically Endangered Bird. *Current Biology, 29*(16), 2711-2717.e2714. doi:10.1016/j.cub.2019.06.064

Hedrick, P. W., & Garcia-Dorado, A. (2016). Understanding Inbreeding Depression, Purging, and Genetic Rescue. *Trends in Ecology & Evolution, 31*(12), 940-952. doi:10.1016/j.tree.2016.09.005

Hedrick, P. W., Kardos, M., Peterson, R. O., & Vucetich, J. A. (2017). Genomic Variation of Inbreeding and Ancestry in the Remaining Two Isle Royale Wolves. *Journal of Heredity, 108*(2), 120-126. doi:10.1093/jhered/esw083

Hillestad, B., Woolliams, J. A., Boison, S. A., Grove, H., Meuwissen, T., Vage, D. I., & Klemetsdal, G. (2017). Detection of runs of homozygosity in Norwegian Red: Density, criteria and genotyping quality control. *Acta Agriculturae Scandinavica Section A - Animal Science, 67*(3-4), 107-116. doi:10.1080/09064702.2018.1501088

Hoffman, J. I., Simpson, F., David, P., Rijks, J. M., Kuiken, T., Thorne, M. A. S., . . . Dasmahapatra, K. K. (2014). High-throughput sequencing reveals inbreeding depression in a natural population. *Proceedings of the National Academy of Sciences, 111*(10), 3775-3780. doi:10.1073/pnas.1318945111

Hoffmann, A. A., Sgro, C. M., & Kristensen, T. N. (2017). Revisiting Adaptive Potential, Population Size, and Conservation. *Trends in Ecology & Evolution, 32*(7), 506-517. doi:10.1016/j.tree.2017.03.012

Hooper, R., Excoffier, L., Forney, K. A., Gilbert, M. T. P., Martin, M. D., Morin, P. A., . . . Foote, A. D. (2020). Runs of homozygosity in killer whale genomes provide a global record of demographic histories. *bioRxiv*, 2020.2004.2008.031344. doi:10.1101/2020.04.08.031344

Hubley, R., Finn, R. D., Clements, J., Eddy, S. R., Jones, T. A., Bao, W., . . . Wheeler, T. J. (2016). The Dfam database of repetitive DNA families. *Nucleic acids research, 44*(D1), D81-89. doi:10.1093/nar/gkv1272

Huisman, J., Kruuk, L. E., Ellis, P. A., Clutton-Brock, T., & Pemberton, J. M. (2016a). Inbreeding depression across the lifespan in a wild mammal population. *Proceedings of the National Academy of Sciences, 113*(13), 3585-3590. doi:10.1073/pnas.1518046113

Huisman, J., Kruuk, L. E., Ellis, P. A., Clutton-Brock, T., & Pemberton, J. M. (2016b). Inbreeding depression across the lifespan in a wild mammal population. *Proc Natl Acad Sci U S A, 113*(13), 3585-3590. doi:10.1073/pnas.1518046113

Humble, E., Paijmans, A. J., Forcada, J., & Hoffman, J. I. (2020). An 85K SNP Array Uncovers Inbreeding and Cryptic Relatedness in an Antarctic Fur Seal Breeding Colony. *G3: Genes|Genomes|Genetics, 10*(8), 2787. doi:10.1534/g3.120.401268

Kardos, M., Akesson, M., Fountain, T., Flagstad, O., Liberg, O., Olason, P., . . . Ellegren, H. (2018a). Genomic consequences of intensive inbreeding in an isolated wolf population. *Nature Ecology & Evolution, 2*(1), 124-131. doi:10.1038/s41559-017-0375-4

Kardos, M., Nietlisbach, P., & Hedrick, P. W. (2018b). How should we compare different genomic estimates of the strength of inbreeding depression? *Proceedings of the National Academy of Sciences, 115*(11), E2492-E2493. doi:10.1073/pnas.1714475115

Kardos, M., Qvarnstrom, A., & Ellegren, H. (2017). Inferring Individual Inbreeding and Demographic History from Segments of Identity by Descent in *Ficedula* Flycatcher Genome Sequences. *Genetics, 205*(3), 1319-1334. doi:10.1534/genetics.116.198861

Kardos, M., Taylor, H. R., Ellegren, H., Luikart, G., & Allendorf, F. W. (2016). Genomics advances the study of inbreeding depression in the wild. *Evolutionary Applications, 9*(10), 1205-1218. doi:10.1111/eva.12414

Keller, M. C., Visscher, P. M., & Goddard, M. E. (2011). Quantification of inbreeding due to distant ancestors and its detection using dense single nucleotide polymorphism data. *Genetics, 189*(1), 237-249. doi:10.1534/genetics.111.130922

Kirin, M., McQuillan, R., Franklin, C. S., Campbell, H., McKeigue, P. M., & Wilson, J. F. (2010). Genomic Runs of Homozygosity Record Population History and Consanguinity. *PLoS One, 5*(11), e13996. doi:10.1371/journal.pone.0013996

Knief, U., Hemmrich-Stanisak, G., Wittig, M., Franke, A., Griffith, S. C., Kempenaers, B., & Forstmeier, W. (2015). Quantifying realized inbreeding in wild and captive animal populations. *Heredity, 114*, 397-403. doi:10.1038/hdy.2014.116

Kolmogorov, M., Yuan, J., Lin, Y., & Pevzner, P. A. (2019). Assembly of long, error-prone reads using repeat graphs. *Nature Biotechnology, 37*(5), 540-546. doi:10.1038/s41587-019-0072-8

Leutenegger, A.-L., Prum, B., Génin, E., Verny, C., Lemainque, A., Clerget-Darpoux, F., & Thompson, E. A. (2003). Estimation of the Inbreeding Coefficient through Use of Genomic Data. *The American Journal of Human Genetics, 73*(3), 516-523. doi:10.1086/378207

Li, H. (2013). Aligning sequence reads, clone sequences and assembly contigs with BWA-MEM. *arXiv preprint arXiv:1303.3997*.

Li, H. (2018). Minimap2: pairwise alignment for nucleotide sequences. *Bioinformatics, 34*(18), 3094-3100. doi:10.1093/bioinformatics/bty191

Li, H., Handsaker, B., Wysoker, A., Fennell, T., Ruan, J., Homer, N., . . . Genome Project Data Processing Subgroup. (2009). The Sequence Alignment/Map format and SAMtools. *Bioinformatics, 25*(16), 2078-2079. doi:10.1093/bioinformatics/btp352

Marshall, T. C., & Spalton, J. A. (2000). Simultaneous inbreeding and outbreeding depression in reintroduced Arabian oryx. *Animal Conservation, 3*(3), 241-248. doi:10.1111/j.1469-1795.2000.tb00109.x

Maya-Garcia, R., Arizaga, S., Cuevas-Reyes, P., Penaloza-Ramirez, J. M., Ramirez, V. R., & Oyama, K. (2017). Landscape genetics reveals inbreeding and genetic bottlenecks in the extremely rare short-globose cacti *Mammillaria pectinifera* (Cactaceae) as a result of habitat fragmentation. *Plant Diversity, 39*(1), 13-19. doi:10.1016/j.pld.2016.09.005

McLennan, E. A., Wright, B. R., Belov, K., Hogg, C. J., & Grueber, C. E. (2019). Too much of a good thing? Finding the most informative genetic data set to answer conservation questions. *Molecular Ecology Resources, 19*(3), 659-671. doi:10.1111/1755-0998.12997

McMahon, B. J., Teeling, E. C., & Hoglund, J. (2014). How and why should we implement genomics into conservation? *Evolutionary Applications, 7*(9), 999-1007. doi:10.1111/eva.12193

McQuillan, R., Leutenegger, A. L., Abdel-Rahman, R., Franklin, C. S., Pericic, M., Barac-Lauc, L., . . . Wilson, J. F. (2008). Runs of homozygosity in European populations. *American Journal of Human Genetics, 83*(3), 359-372. doi:10.1016/j.ajhg.2008.08.007

Meyermans, R., Gorssen, W., Buys, N., & Janssens, S. (2020). How to study runs of homozygosity using PLINK? A guide for analyzing medium density SNP data in livestock and pet species. *BMC Genomics, 21*(1), 94. doi:10.1186/s12864-020-6463-x

Minias, P., Dunn, P. O., Whittingham, L. A., Johnson, J. A., & Oyler-McCance, S. J. (2019). Evaluation of a Chicken 600K SNP genotyping array in non-model species of grouse. *Scientific Reports, 9*(1), 6407. doi:10.1038/s41598-019-42885-5

Narum, S. R., Buerkle, C. A., Davey, J. W., Miller, M. R., & Hohenlohe, P. A. (2013). Genotyping-by-sequencing in ecological and conservation genomics. *Molecular Ecology, 22*(11), 2841-2847. doi:10.1111/mec.12350

Niskanen, A. K., Billing, A. M., Holand, H., Hagen, I. J., Araya-Ajoy, Y. G., Husby, A., . . . Jensen, H. (2020). Consistent scaling of inbreeding depression in space and time in a

house sparrow metapopulation. *Proceedings of the National Academy of Sciences, 117*(25), 14584-14592. doi:10.1073/pnas.1909599117

Parlato, E. H., Ewen, J. G., McCready, M., Parker, K. A., & Armstrong, D. P. (2021). A modelling framework for integrating reproduction, survival and count data when projecting the fates of threatened populations. *Oecologia, 195*(3), 627-640. doi:10.1007/s00442-021-04871-5

Pemberton, J. M. (2008). Wild pedigrees: the way forward. *Proceedings of the Royal Society B: Biological Sciences, 275*(1635), 613-621. doi:10.1098/rspb.2007.1531

Pemberton, T. J., Absher, D., Feldman, M. W., Myers, R. M., Rosenberg, N. A., & Li, J. Z. (2012). Genomic patterns of homozygosity in worldwide human populations. *American Journal of Human Genetics, 91*(2), 275-292. doi:10.1016/j.ajhg.2012.06.014

Poplin, R., Ruano-Rubio, V., DePristo, M. A., Fennell, T. J., Carneiro, M. O., Van der Auwera, G. A., . . . Banks, E. (2018). Scaling accurate genetic variant discovery to tens of thousands of samples. *bioRxiv*, 201178. doi:10.1101/201178

Pryce, J. E., Haile-Mariam, M., Goddard, M. E., & Hayes, B. J. (2014). Identification of genomic regions associated with inbreeding depression in Holstein and Jersey dairy cattle. *Genetics Selection Evolution, 46*(1), 71. doi:10.1186/s12711-014-0071-7

Puckett, E. E. (2017). Variability in total project and per sample genotyping costs under varying study designs including with microsatellites or SNPs to answer conservation genetic questions. *Conservation Genetics Resources, 9*(2), 289-304. doi:10.1007/s12686-016-0643-7

Purfield, D. C., McParland, S., Wall, E., & Berry, D. P. (2017). The distribution of runs of homozygosity and selection signatures in six commercial meat sheep breeds. *PLoS One, 12*(5), e0176780. doi:10.1371/journal.pone.0176780

R Core Team. (2013). R: A language and environment for statistical computing: Vienna, Austria. Retrieved from http://www.R-project.org/

Robinson, J. A., Räikkönen, J., Vucetich, L. M., Vucetich, J. A., Peterson, R. O., Lohmueller, K. E., & Wayne, R. K. (2019). Genomic signatures of extensive inbreeding in Isle Royale wolves, a population on the threshold of extinction. *Science Advances, 5*(5), eaau0757. doi:10.1126/sciadv.aau0757

Saremi, N. F., Supple, M. A., Byrne, A., Cahill, J. A., Coutinho, L. L., Dalen, L., . . . Shapiro, B. (2019). Puma genomes from North and South America provide insights into the genomic consequences of inbreeding. *Nature Communications, 10*(1), 4769. doi:10.1038/s41467-019-12741-1

Schiavo, G., Bovo, S., Bertolini, F., Dall'Olio, S., Costa, L. N., Tinarelli, S., . . . Fontanesi, L. (2020). Runs of homozygosity islands in Italian cosmopolitan and autochthonous pig breeds identify selection signatures in the porcine genome. *Livestock Science, 240*, 104219. doi:10.1016/j.livsci.2020.104219

Shafer, A. B. A., Miller, J. M., & Kardos, M. (2016). Cross-Species Application of SNP Chips is Not Suitable for Identifying Runs of Homozygosity. *Journal of Heredity, 107*(2), 193-195. doi:10.1093/jhered/esv137

Simao, F. A., Waterhouse, R. M., Ioannidis, P., Kriventseva, E. V., & Zdobnov, E. M. (2015). BUSCO: assessing genome assembly and annotation completeness with single-copy orthologs. *Bioinformatics, 31*(19), 3210-3212. doi:10.1093/bioinformatics/btv351

Slate, J., David, P., Dodds, K. G., Veenvliet, B. A., Glass, B. C., Broad, T. E., & McEwan, J. C. (2004). Understanding the relationship between the inbreeding coefficient and multilocus heterozygosity: theoretical expectations and empirical data. *Heredity, 93*(3), 255-265. doi:10.1038/sj.hdy.6800485

Slate, J., Kruuk, L. E. B., Marshall, T. C., Pemberton, J. M., & Clutton-Brock, T. H. (2000). Inbreeding depression influences lifetime breeding success in a wild population of red deer (Cervus elaphus). *Proceedings of the Royal Society of London. Series B: Biological Sciences, 267*(1453), 1657-1662. doi:10.1098/rspb.2000.1192

Smit, A., Hubley, R., & Green, P. (2015a). RepeatMasker Open-4.0. 2013–2015.

Smit, A., Hubley, R., & Green, P. (2015b). RepeatModeler Open-1.0. 2008–2015.

Sölkner, J., Ferencakovic, M., Gredler, B., & Curik, I. (2010). *Genomic metrics of individual autozygosity, applied to a cattle population.* Paper presented at the Book of Abstracts of the 61st Annual Meeting of the European Association of Animal Production.

Stoffel, M. A., Esser, M., Kardos, M., Humble, E., Nichols, H., David, P., & Hoffman, J. I. (2016). inbreedR: an R package for the analysis of inbreeding based on genetic markers. *Methods in Ecology and Evolution, 7*(11), 1331-1339. doi:10.1111/2041-210x.12588

Stoffel, M. A., Johnston, S. E., Pilkington, J. G., & Pemberton, J. M. (in press). Mutation load decreases with haplotype age in wild Soay sheep. *Evolution Letters*. doi:doi.org/10.1002/evl3.229

Szpiech, Z. A., Xu, J., Pemberton, T. J., Peng, W., Zollner, S., Rosenberg, N. A., & Li, J. Z. (2013). Long runs of homozygosity are enriched for deleterious variation. *American Journal of Human Genetics, 93*(1), 90-102. doi:10.1016/j.ajhg.2013.05.003

van der Valk, T., Gonda, C. M., Silegowa, H., Almanza, S., Sifuentes-Romero, I., Hart, T. B., . . . Guschanski, K. (2019). The Genome of the Endangered Dryas Monkey Provides New Insights into the Evolutionary History of the Vervets. *Molecular Biology and Evolution, 37*(1), 183-194. doi:10.1093/molbev/msz213

Vendrami, D. L. J., Houston, R. D., Gharbi, K., Telesca, L., Gutierrez, A. P., Gurney-Smith, H., . . . Hoffman, J. I. (2019). Detailed insights into pan-European population structure and inbreeding in wild and hatchery Pacific oysters (*Crassostrea gigas*) revealed by genome-wide SNP data. *Evolutionary Applications, 12*(3), 519-534. doi:10.1111/eva.12736

Wang, P., Burley, J. T., Liu, Y., Chang, J., Chen, D., Lu, Q., . . . Zhang, Z. (2021). Genomic Consequences of Long-Term Population Decline in Brown Eared Pheasant. *Molecular Biology and Evolution, 38*(1), 263-273. doi:10.1093/molbev/msaa213

Weeks, A. R., Sgro, C. M., Young, A. G., Frankham, R., Mitchell, N. J., Miller, K. A., . . . Hoffmann, A. A. (2011). Assessing the benefits and risks of translocations in changing environments: a genetic perspective. *Evolutionary Applications, 4*(6), 709-725. doi:10.1111/j.1752-4571.2011.00192.x

Wick, R. R., Judd, L. M., Gorrie, C. L., & Holt, K. E. (2017). Completing bacterial genome assemblies with multiplex MinION sequencing. *Microbial genomics, 3*(10), e000132. doi:10.1099/mgen.0.000132

Xue, Y., Prado-Martinez, J., Sudmant, P. H., Narasimhan, V., Ayub, Q., Szpak, M., . . . Scally, A. (2015). Mountain gorilla genomes reveal the impact of long-term population decline and inbreeding. *Science, 348*(6231), 242-245. doi:10.1126/science.aaa3952

Yang, J., Lee, S. H., Goddard, M. E., & Visscher, P. M. (2011). GCTA: A Tool for Genome-wide Complex Trait Analysis. *The American Journal of Human Genetics, 88*(1), 76-82. doi:10.1016/j.ajhg.2010.11.011

Yoshida, G. M., Caceres, P., Marin-Nahuelpi, R., Koop, B. F., & Yanez, J. M. (2020). Estimates of Autozygosity Through Runs of Homozygosity in Farmed Coho Salmon. *Genes, 11*(5), 490. doi:10.3390/genes11050490

Zhang, X., Deng, C., Ding, J., Ren, Y., Zhao, X., Qin, S., . . . Zhu, L. (2016). Comparative genomics and metagenomics analyses of endangered Père David's deer (*Elaphurus davidianus*) provide insights into population recovery. *bioRxiv*, 073528. doi:10.1101/073528

Zhao, S., Zheng, P., Dong, S., Zhan, X., Wu, Q., Guo, X., . . . Wei, F. (2013). Whole-genome sequencing of giant pandas provides insights into demographic history and local adaptation. *Nature Genetics, 45*(1), 67-71. doi:10.1038/ng.2494

Zilko, J. P., Harley, D., Hansen, B., Pavlova, A., & Sunnucks, P. (2020). Accounting for cryptic population substructure enhances detection of inbreeding depression with

genomic inbreeding coefficients: an example from a critically endangered marsupial. *Molecular Ecology, 29*(16), 2978-2993. doi:10.1111/mec.15540

In prep:

Lee, K.D., Millar, C.D., Brekke, P., Whibley A., Ewen, J.G., Hingston, M., Zhu, A., and Santure, A.W. In preparation. The design and application of a 50K SNP microarray for a threatened Aotearoa New Zealand passerine, the hihi.
Provided as an additional file for review only.

Data accessibility and Benefit-Sharing Statement

Hihi are of cultural significance to the indigenous people of New Zealand, the Māori, and are considered a taonga (treasured) species whose whakapapa (genealogy) is intricately tied to that of Māori. For this reason, the raw reads, assembly and genotypes for hihi will be made available by request on the recommendation of Ngāti Manuhiri, the iwi (tribe) that affiliates as kaitiaki (guardians) for hihi. To obtain contact details for the iwi, please contact Dr Anna Santure: a.santure@auckland.ac.nz.

Author contributions

LD, A.W.S. and A.C.W. designed the study. A.C.W. generated and assembled the reference genome, repeat-masked the assembly, called genotypes in the reference individual and mapped resequencing, RAD-seq and SNP array SNPs to the genome for the ten individuals. L.D. designed and conducted all inbreeding analyses, with advice from A.W.S. L.D. produced the figures and wrote the paper with input from all authors. P.B. and J.G.E. coordinated the hihi sampling. All authors commented on and approved the final manuscript.

Tables and Figures

Table 2: *Output from the ROH analysis in PLINK for the assembly male Yellow. Each dataset has been scanned for runs of homozygosity ≥300kb using custom parameters depending on SNP density. Displayed are: the total number of genotyped sites, the genome coverage parameter, the number of these sites detected within an ROH, the percentage of SNPs that are also in a run when scanning the full genome, the percentage of SNPs that are also outside a ROH when scanning the full genome, the total number of ROH found, the total length of all ROH in kb, inbreeding (F_{ROH}) estimated as the total length of detected runs divided by the sum of contigs larger than the minimum ROH size of 300kb and F_{ROH} when considering ROHs of ≥500kb. Detailed PLINK ROH settings in Supplementary Methods and Supplementary Tables S2 and S3.*

	Full genome	Combined	WGS	SNP array	RAD-seq
Genotyped sites	904,228,112	1,593,073	1,562,384	46,136	18,415
Genome coverage parameter		98.3%	98.3%	93.4%	54.2%
#sites in ROH	176,447,917	263,068	290,384	11,421	6,021
% agreement with full genome on ROH exclusion		96.0%	97.1%	81.0%	62.7%
% agreement with full genome on ROH inclusion		95.9%	95.4%	88.1%	72.5%
Total # of ROH	270	290	300	223	285
Total length (kb)	201,000	199,335	207,481	236,390	186,613
F_{ROH} (≥ 300kb)	0.202	0.192	0.199	0.227	0.179
F_{ROH} (≥ 500kb)	0.149	0.138	0.144	0.224	0.130

Figure 1: Two example contigs (#275 and #347) showing the detection of runs of homozygosity for the genome individual Yellow using different marker densities. Positions in light blue were not involved in a ROH, while positions in dark red (#275) and dark blue (#347) were. For each contig, (A) denotes full genome sequence, (B) denotes the combined SNP dataset based on heterozygote calls in the dataset, and inferred genotypes at lcWGS, SNP-array and RAD-seq positions, (C) denotes inferred SNP-array genotypes, (D) denotes inferred RAD-seq genotypes.

Figure 2: The number and total length of ROH found, the percentage of SNPs that are also in a run when scanning the combined dataset (% agreement on inclusion) and the percentage of SNPs that are also outside a ROH when scanning the combined dataset (% agreement on exclusion), when randomly down-sampling the combined dataset

that was generated for the male hihi. The number of variants are displayed on a log scale. The array and RAD-seq densities were i) generated via random down-sampling to the same total number (grey dots) but also ii) displayed with real RAD-seq and SNP array positions (the latter labelled in red). Note that the high % agreement on exclusion for the two smallest datasets are due to these datasets detecting very few ROHs; these failures to detect ROHs are reflected in the low % agreement on inclusion. The trend line was plotted with the geom_smooth(method = "loess") function in ggplot2 in R. Detailed PLINK ROH settings in Supplementary Material and Supplementary Tables S2-S5.

Figure 3*: Location of runs of homozygosity (ROH) for one example contig (#436) that had ROH detected across all seven datasets, with ROH landscapes shown for the RAD-seq, SNP array and lcWGS8 datasets. Displayed are the percentage of the ten birds (y-axis) that have this SNP (x-axis) involved in a run of homozygosity. The more individuals share the ROH, the higher the SNP is located in the plot. Red dots at the bottom of the plot mean that those SNPs were not involved in a ROH in any bird. ROH for the other datasets shown in Supplementary Figure S3, SNPs in HBD segments according to RZooRoH shown in Supplementary Figure S4.*